

This article was downloaded by:

On: 15 January 2011

Access details: *Access Details: Free Access*

Publisher *Taylor & Francis*

Informa Ltd Registered in England and Wales Registered Number: 1072954 Registered office: Mortimer House, 37-41 Mortimer Street, London W1T 3JH, UK



Comments on Inorganic Chemistry

Publication details, including instructions for authors and subscription information:

<http://www.informaworld.com/smpp/title~content=t713455155>

METALLOPHILIC INTERACTIONS IN DOUBLE SALTS: TOWARD 1D METAL ATOM CHAINS

Linda H. Doerrera

^a Chemistry Department, Boston University, Boston, Massachusetts, USA

To cite this Article Doerrera, Linda H.(2008) 'METALLOPHILIC INTERACTIONS IN DOUBLE SALTS: TOWARD 1D METAL ATOM CHAINS', *Comments on Inorganic Chemistry*, 29: 3, 93 — 127

To link to this Article: DOI: 10.1080/02603590802310760

URL: <http://dx.doi.org/10.1080/02603590802310760>

PLEASE SCROLL DOWN FOR ARTICLE

Full terms and conditions of use: <http://www.informaworld.com/terms-and-conditions-of-access.pdf>

This article may be used for research, teaching and private study purposes. Any substantial or systematic reproduction, re-distribution, re-selling, loan or sub-licensing, systematic supply or distribution in any form to anyone is expressly forbidden.

The publisher does not give any warranty express or implied or make any representation that the contents will be complete or accurate or up to date. The accuracy of any instructions, formulae and drug doses should be independently verified with primary sources. The publisher shall not be liable for any loss, actions, claims, proceedings, demand or costs or damages whatsoever or howsoever caused arising directly or indirectly in connection with or arising out of the use of this material.

METALLOPHILIC INTERACTIONS IN DOUBLE SALTS: TOWARD 1D METAL ATOM CHAINS

LINDA H. DOERRER

Chemistry Department, Boston University, Boston,
Massachusetts, USA

A new family of double salts has been developed that can display infinite one-dimensional chains of metallophilic interactions in the solid state. These salts are composed of cationic and anionic components that are designed to participate in metallophilic interactions with one another. These building blocks incorporate Au(III), Au(I), and Pt(II) atoms in the forms $[L_3PtX]^+$, $[L_2AuX_2]^+$, $[AuX_4]^-$, and $[AuX_2]^-$. Five different metallophilic structural motifs have been observed in these double salts and their monomeric precursors. The particular structure observed is affected by metal oxidation state, the electronic nature of the neutral (L) and anionic (X) substituents, the synthetic conditions employed, as well as the solvent present.

1D STRUCTURES

Many extended lattice systems such as elemental metals or common salts and minerals have similar bonding interactions in all three spatial dimensions and therefore isotropic chemical and physical properties. More rare are systems where there are gaps in the bonding in one dimension but strong bonding in the remaining two. Graphite is the archetype of these planar structures that also includes such compounds as layered bronzes of molybdenum or tungsten.^[1] The high T_c superconductors are layered oxides whose fascinating behavior seems tied to the

Address corresponding to Linda H. Doerrer, Chemistry Department, Boston University, 590 Commonwealth Ave., Boston, MA 02215, USA. E-mail: doerrer@bu.edu

two-dimensional (2D) behavior of the electrons.^[2] The most anisotropic systems with significant bonding in only one dimension are even more rare.

These highly anisotropic organic (including transition metal organometallic or coordination compounds) and inorganic (primarily metal oxides) one-dimensional (1D) solids are the subject of intense and enduring interest. They are important test-beds for understanding quantum physics in reduced dimensions, they display complex electron correlation effects, and single chain magnets can behave as anisotropic Ising ferro- or ferrimagnetic systems.^[3,4] These materials also have potentially useful physical properties including anisotropic electrical conduction and enhanced non-linear optical behavior.^[5] Although low dimensional organic materials can display different broken-symmetry ground states such as charge density waves, spin density waves, Peierls or spin-Peierls distortions, and superconductivity, it is difficult to predict which properties will be observed from the composition or structure of the material.^[6] There is much room for the development of structure-function relationships in the field of organic conductors. Conducting 1D materials could be of particular use in nanoscale electronic devices as interconnects or for use in nanoscale photovoltaic devices that require efficient charge separation through a conducting molecular path.

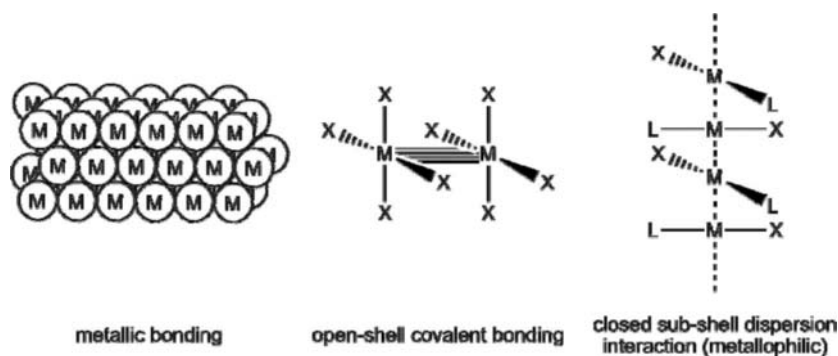
Toward this end, we are interested in preparing compounds that have an effectively infinite chain of metal atoms surrounded by an insulating coat. Such a structure could function as a molecular wire if the right contacts are made on both ends and the electronic occupation of the metal-based orbitals is tailored appropriately. Our group has used a general synthetic approach to develop double salts with precious metals. These salts are intellectually descended from the all-platinum progenitor $[\text{Pt}(\text{NH}_3)_4]^{2+}[\text{PtCl}_4]^{2-}$, also known as Magnus' green salt,^[7-10] and other similar $[\text{Pt}(\text{II})]^{2+}[\text{Pt}(\text{II})]^{2-}$ systems including the $[\text{Pt}(\text{NH}_2\text{R})_4]^{2+}[\text{PtCl}_4]^{2-}$ compounds developed by the Caseri group^[11] and the $[\text{Pt}(\text{CNR})_4]^{2+}[\text{Pt}(\text{CN})_4]^{2-}$ salts from the Mann group.^[12,13]

We intended to improve on these systems in several ways including (i) using cation and anion building blocks with single positive or negative charges for greater solubility, (ii) using more lipophilic ligand groups also to facilitate solubility and greater ease of materials processing, and (iii) developing families of cations and anions that could be mixed combinatorially and create a large number of salts for comparative study of

electronic properties including structure-property relationships. Our initial results are described in this review and utilize not only d^8 Pt(II)- but also d^8 Au(III)- and d^{10} Au(I)-containing ions. In recent decades these metals with these electronic configurations have been observed to form metal-metal bonding-type interactions with one another in a legion of small molecules. We have chosen to use these so-called *metallophilic* interactions as a central design element for our nanowires.

METALLOPHILICITY

Bonding between metal atoms may be divided into three different general types as depicted in Scheme 1: (i) metallic bonding among the elements as well described by band structure and Fermi surface concepts.^[14,15] (ii) bonding between oxidized metal atoms with open subshells as exemplified by the d^4 Re(III) centers in $[\text{Re}_2\text{Cl}_8]^{2-}$.^[16] and (iii) bonding between metal atoms with closed subshell configurations such as d^{10} or s^2 .^[17] This third category is the most recent to be observed and encompasses some unusual structure types that are counterintuitive at first glance. The bonding is termed *metallophilic* because the metal-metal interactions do not involve traditional sharing of electrons in covalent bonds nor the sharing of delocalized electrons via a conduction band. Rather the metals have an affinity for one another not driven by electrostatics, covalently shared electrons, or closest packing of spheres. These interactions are identified most commonly in single crystal X-ray diffraction data when two metal centers are closer to one another than

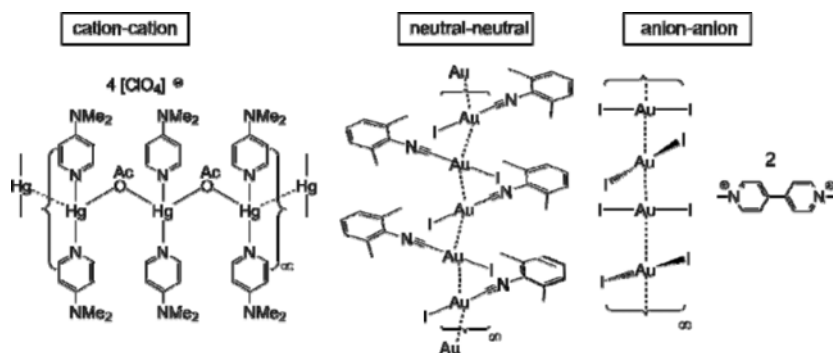


Scheme 1. Metal-metal bonding types: metallic (left), covalent (center), and metallophilic (right).

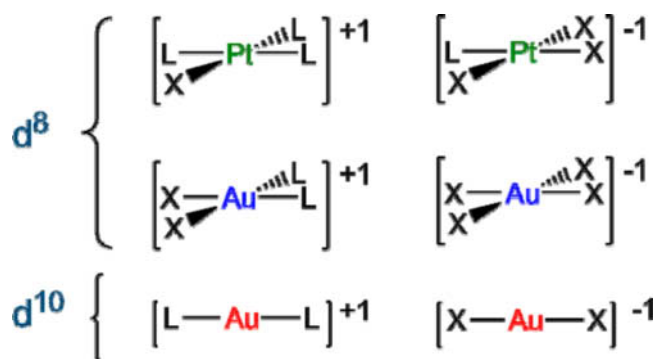
the sum of their van der Waals radii.^[18] The energies of the metallophilic interactions are on the order of hydrogen-bonding^[17,19] and are therefore a significant determinant of the ground state geometry. Metallophilic bonding is understood^[17] as a type of dispersion interaction between two metal centers that have d^8 , d^{10} , or s^2 valence shell configurations. Calculations at the Hartree-Fock level in d^{10} cases that include mixing of occupied d_{z^2} and unoccupied s and/or p_z orbitals cannot account for the energetic stabilization of metallophilic interactions.^[20,21] Only when configuration interactions are also included^[22–24] are the experimental structures correctly reproduced computationally.

Metallophilic interactions were first observed in gold-containing complexes and termed aurophilic interactions.^[25,26] Since that time, they have been observed within hundreds of transition metal compounds that contain nd^8 , nd^{10} , or $nd^{10}(n+1)s^2$ electronic configurations. They are observed, as shown in Scheme 2, between neutral species,^[27] but also between cations^[28] or between anions.^[29] This latter phenomenon of bringing together charged moieties in opposition to coulombic forces without formation of a covalent bond is unique to metallophilic interactions.

We have selected Pt- and Au-containing ions for our initial studies because third-row transition metals with d^8 and d^{10} configurations have strong ligand field stabilization energies leading to robust square planar coordination for Au(III) and Pt(II), and linear geometries for Au(I). Because salt solubility is inversely proportional to the charge on the



Scheme 2. Examples of metallophilic interactions between cations (left), neutral species (center), and anions (right).



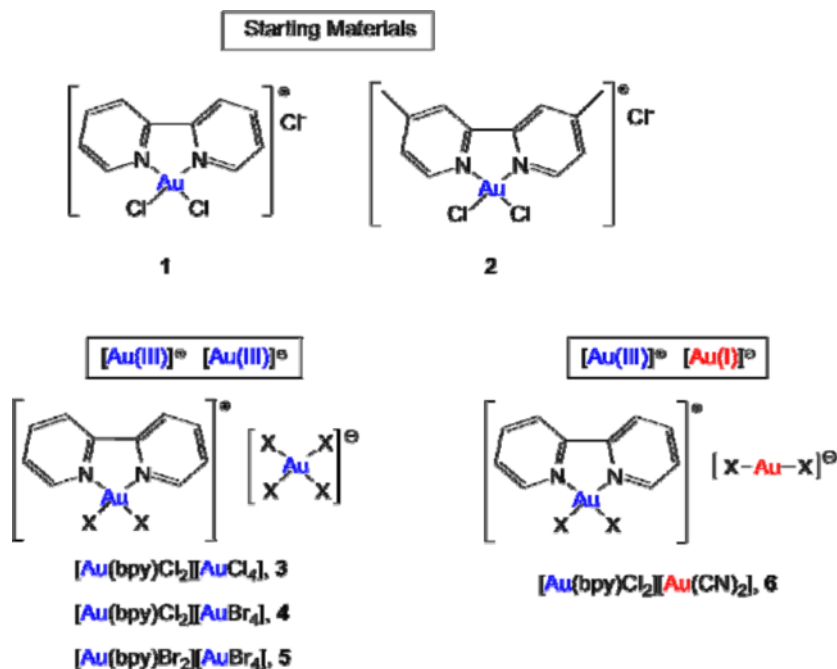
Scheme 3. Cations and anions for metallophilic double salts with MLXZ ligand descriptions.

component ions, we have chosen to work predominantly with monovalent cations and anions. Using the MLXZ classification scheme,^[30] the target cations and anions are represented as shown in Scheme 3 below. Bipyridine (L_2) and terpyridine (L_3) were selected as neutral ligands whose chemistry fit in well with all the requirements for our system. A review of terpyridine chemistry with Pd(II), Pt(II) and Au(III) metal ions has recently appeared.^[31]

Combination of these cations and anions in a 1:1 ratio results in double salts that are held together by coulombic forces as well as metallophilic ones. The preferred method for making these double salts is a metathesis reaction between appropriately chosen salts in a solvent in which only one of the products is soluble. The two products are readily separated via filtration, and the double salt can be recrystallized subsequently for further purification. Aqueous reactions are particularly favorable when KCl is one product and the other is a double salt insoluble in water, but readily recrystallized from polar organic solvents. In the cases where water caused additional reactivity to occur, alternative procedures were developed.

GOLD COMPOUNDS: SYNTHESIS AND STRUCTURAL CHARACTERIZATION

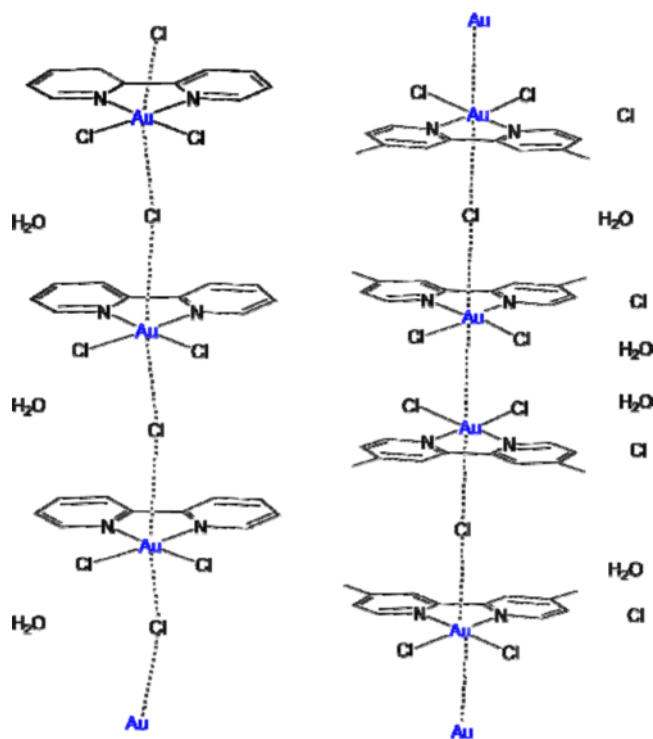
The first compound used in our gold studies was $[\text{Au}(\text{bpy})\text{Cl}_2]\text{Cl}$, 1. The gold-containing starting materials and a summary of the double salts with gold cations are shown in Scheme 4.



Scheme 4. Summary of gold-containing cation starting materials and double-salt compounds.

Compound **1** was originally reported in the literature almost fifty years ago.^[32] The crystal structure^[33] of this derivative had not been reported prior to our work, although both $[\text{Au}(\text{bpy})\text{Cl}_2](\text{NO}_3)$ ^[34] and $[\text{Au}(\text{bpy})\text{Cl}_2](\text{BF}_4)$ ^[35] had been structurally characterized. No metallophilic interactions are present in $[\text{Au}(\text{bpy})\text{Cl}_2]\text{Cl}\cdot\text{H}_2\text{O}$ ^[33] or either of the other two $[\text{Au}(\text{bpy})\text{Cl}_2]^+$ structures. We prepared the analogous $[\text{Au}(\text{Me}_2\text{bpy})\text{Cl}]\text{Cl}$ derivative, **2**, and also determined the crystal structure.^[36] A comparison of these two $[\text{Au}(\text{R}_2\text{bpy})\text{Cl}_2]\text{Cl}$ structures is shown in Scheme 5. In the non-alkylated derivative, the cations and anions alternate and there are no remotely close $\text{Au}\cdots\text{Au}$ contacts. The $\text{Au}-\text{Cl}$ distance for the bridging chlorides is 3.183 Å, which is well beyond the average $\text{Au(III)}-\text{Cl}$ single bond length of 2.315(5) Å reported in the Cambridge Structural Database (CSD).^[37]

In contrast, in the structure of **2** half of the chloride ions do not participate in electrostatic interactions with cations, but are outside



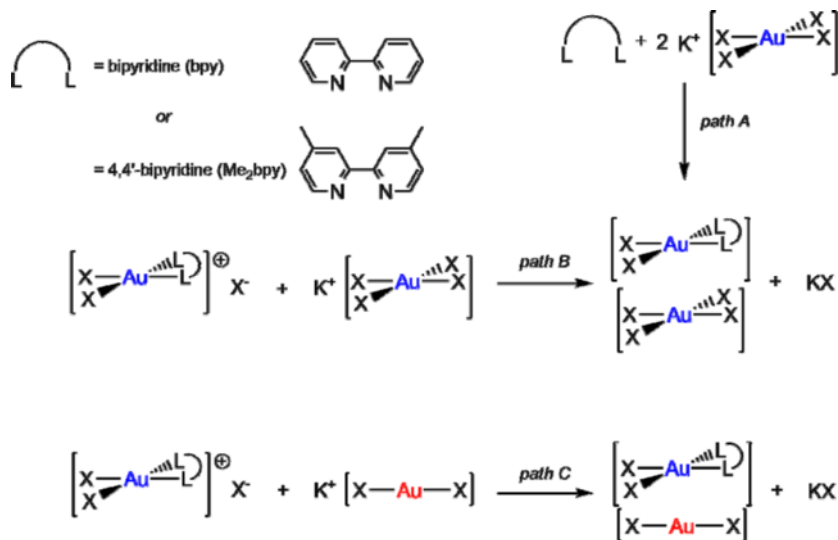
Scheme 5. Comparison of stacking patterns in 1 (left) and 2 (right).

$\{\text{Au}_2\text{Cl}\}_\infty$ chains formed by metallophilic interactions and participate only in hydrogen bonding with the lattice water molecules. In 2, the cations interact pairwise through aurophilic contacts at a distance of 3.587 Å. This distance is long for Au-Au metallophilic interactions, but is consistent with the few other Au(III)···Au(III) distances reported in the literature.^[38,39] The Au(III)···Au(III) aurophilic interaction had been postulated based on computational studies,^[24] and was only experimentally characterized for the first time recently. The first Au(III)···Au(III) interaction was reported in chains of the $[\text{Au}(\text{N}_3)_4]^-$ anions,^[38] prepared as the $(\text{Me}_4\text{N})^+$ salt. This chain exhibits a Peierls distortion such that the Au···Au distances alternate between 3.507(3) Å and 3.584(3) Å. The noticeable dependence of Au(III)-Au(III) metallophilic interactions on the 4' methyl groups shows the sensitivity of these

dispersion forces to small changes in electron density at the metal center. Ligand alkylation increases the electron density at gold sufficiently to favor the $\text{Au} \cdots \text{Au}$ interaction in **2** over the $\text{Au} \cdots \text{Cl}$ ones seen in the structure of **1**.

Synthesis of $[\text{Au}(\text{bpy})\text{Br}_2]\text{Br}$ was attempted according to a literature procedure,^[40] however, the compound could not be isolated. The product formed has solubility consistent with the $[\text{Au}(\text{bpy})\text{Br}_2][\text{AuBr}_4]$ double salt, **5**, whose characterization was carried out fully, *vide infra*. This salt may be an intermediate along the route to $[\text{Au}(\text{bpy})\text{Br}_2]\text{Br}$, formed when half of the gold atoms have been coordinated to bipyridine. The double salt precipitates rapidly, however, and does not react further. Alternative methods to the preparation of this compound are under investigation.

Double salts with $\text{Au}(\text{III})$ cations and $\text{Au}(\text{III})$ or $\text{Au}(\text{I})$ anions can be prepared in two ways: (i) by reaction of an $[\text{AuX}_4]^-$ precursor with one half an equivalent of ligand (path A), or (ii) by a metathesis reaction between salts that contain gold-based cations and anions (paths B and C) as shown in Scheme 6. Path A generally leads to salts with the same oxidation state in the cation and anion such as $[\text{Au}(\text{bpy})\text{X}_2][\text{AuX}_4]$, **3** ($\text{X} = \text{Cl}$) or **5** ($\text{X} = \text{Br}$). This method is somewhat limited in scope



Scheme 6. Pathways to $[\text{Au}]^+ [\text{Au}]^-$ double salts.

because the cation and anion will both have the same metal and the anionic ligands are all the same as well. The metathesis reactions, however, have potentially infinite flexibility if the desired cations and anions can be prepared independently. Synthesis of $[\text{Au}]^+[\text{Au}]^-$ double salts in water from $[\text{Au}]^+\text{Cl}^-$ and $\text{K}^+[\text{Au}]^-$ reagents is particularly facile and generally leads to clean precipitation of the double salts while the KCl stays in solution. The double-salt products are recrystallized from strongly polar solvents such as CH_3CN , DMSO, acetone, or DMF. Care must be exercised with these solvents that can engender Au(III) to Au(I) reduction as described below.

The syntheses of $[\text{Au}(\text{bpy})\text{Cl}_2][\text{AuCl}_4]$, **3**, and $[\text{Au}(\text{bpy})\text{Br}_2][\text{AuBr}_4]$, **5**, have been previously reported^[32] but without structural characterization. Subsequent work has been carried out to further characterize both species. Satisfactory elemental analysis data of microcrystalline samples were obtained for both. Crystals suitable for X-ray diffraction experiments could only be obtained from hot CH_3CN solutions, however. Preliminary crystallographic data for nominal $[\text{Au}(\text{bpy})\text{Cl}_2][\text{AuCl}_4]$, **3**, showed linear $\{\text{AuCl}_2\}$ units, which suggested that some in situ reduction of Au(III) to Au(I) had occurred. Definitive evidence for such reduction was obtained in the platinum systems, *vide infra*. A mixed Au(III)/Au(I) system was obtained previously^[41] from HAuCl_4 and terpyridine that yielded the pentanuclear units $\{[\text{Au}(\text{terpy})\text{Cl}][\text{AuCl}_2]_3[\text{Au}(\text{terpy})\text{Cl}]\}^+$ bridged by chlorine atoms from $[\text{AuCl}_4]^-$ groups.

The pursuit for structural data of **5** yielded two crystallographic polymorphs, **5a** and **5b**. The morphology of the two crystals is apparent even on the macroscopic level; **5a** is obtained as long, block-like crystals, whereas **5b** is observed as thin, needle-like crystals. Crystallographic characterization of **5a** shows one formula unit of the double salt in the asymmetric unit (Figure 1, left) with a Au-Au distance of 3.544 Å, which is shorter than the 3.6 Å distance of twice the Au van der Waals radii.^[18] This double salt exhibits the second example of a $\text{Au(III)} \cdots \text{Au(III)}$ metallophilic interaction,^[39] however it does not extend infinitely throughout the crystal (Figure 1, right). The lack of infinite Au-Au contacts may be due to insufficient electron density at the Au(III) centers. Although there is enough electron density in the dimer to provide for one metallophilic interaction, it appears the Au(III) atom in the cationic species requires more electron density than the Au(III) atom in the neighboring anionic species can donate. Instead the Au atom in the cationic species exhibits an interaction with the more electron rich bromide

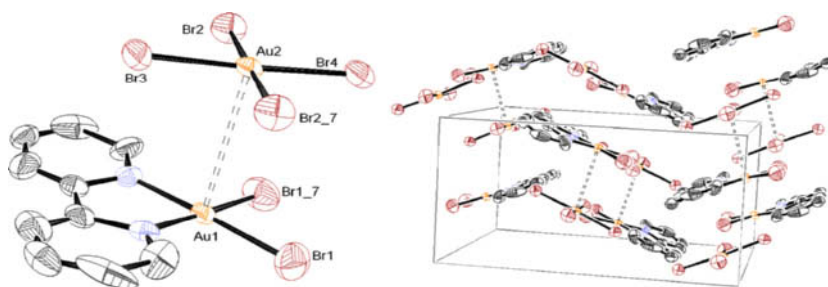


Figure 1. ORTEP representation of **5a** double salt (left) and packing diagram (right) with thermal ellipsoids at 50% level and hydrogen atoms removed for clarity.

ligand on the neighboring dimer's anion (Figure 1, right), similar to the previously discussed $[\text{Au}(\text{terpy})\text{Cl}]_2[\text{AuCl}_2]_3[\text{AuCl}_4]$ structure.^[41] The only reported infinite chain of Au(III) species is that of the $[\text{Au}(\text{N}_3)_4]^-$ anions,^[38] which supports the idea that the greater electron density present in the Au(III)-containing anions favors more metallophilic interactions than between Au(III)-containing cations, as observed in **2**, or between cations and anions, as seen in **5a**.

Interestingly, the **5b** polymorph of $[\text{Au}(\text{bpy})\text{Br}_2][\text{AuBr}_4]$ exhibits no Au-Au interactions in the dimeric unit as shown in Figure 2, right. The cationic Au(III) atom interacts with bromide ligands from the anion

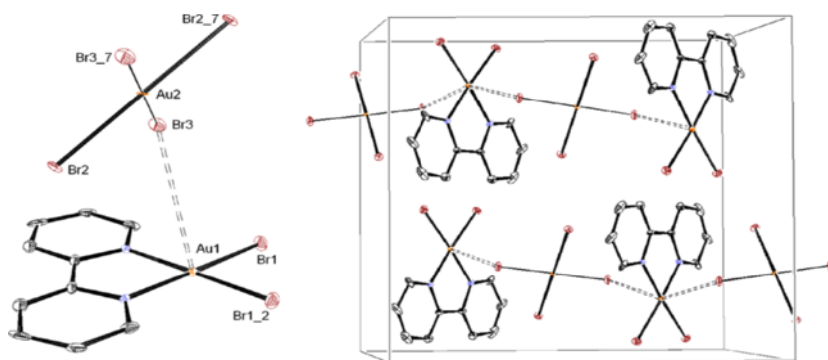


Figure 2. ORTEP representations of $[\text{Au}(\text{bpy})\text{Br}_2][\text{AuBr}_4]$, **5b** salt (left) and packing diagram (right). Thermal ellipsoids are at 50% level and hydrogen atoms removed for clarity.

only. This observation again suggests that when minimal electron density is present on the Au(III) atoms for metallophilic bonding, the cationic Au(III) center prefers to interact with the more electron rich atoms, bromine in this case. The interaction between the bromine and gold atoms is weak, however, as suggested by the lack of lengthening in the Au(2)-Br(3) bond, 2.4232(7) Å, versus the Au(2)-Br(2) bond, 2.4202(6) Å. The right side of Figure 2 shows the pseudo 1D network of (Br...Au) interactions in the crystal lattice. Polymorphs **5a** and **5b** were obtained from the same recrystallization suggesting that the energetic difference of Au or Br coordination from the anion to the Au(III) atom in $[\text{Au}(\text{bpy})\text{Br}_2]^+$ is relatively small. Notably, the **5a** polymorph, exhibiting the metallophilic interaction, is the major product of the recrystallization based on the relative abundances of the two crystal morphologies.

The metathesis method was used to prepare $[\text{Au}(\text{bpy})\text{Cl}_2][\text{AuBr}_4]$, **4**, a mixed halide analog of the homohalogen derivatives **3** and **5**, via the metathesis reaction of **1** and KAuBr_4 . (Scheme 6, path B) The

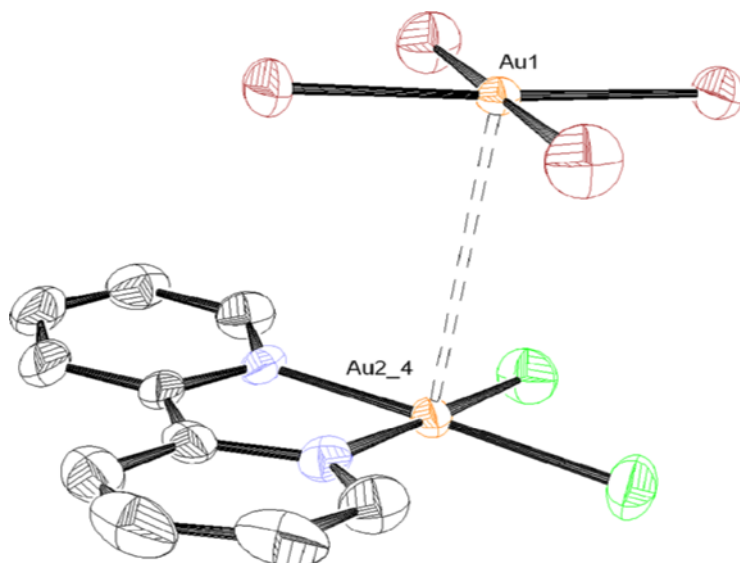


Figure 3. ORTEP of $[\text{Au}(\text{bpy})\text{Cl}_2][\text{AuBr}_4]$, **4**, with 50% thermal ellipsoids and hydrogen atoms removed for clarity.

structural characterization of **4** (Figure 3) exhibits a crystal structure isomorphous to that of **5a**, with similar unit cell dimensions and bond lengths. Compound **4** also contains a metallophilic Au-Au interaction within each dimeric unit only. Again, this structure is attributed to insufficient electron density in the Au(III) cation in the adjacent dimer to drive a metallophilic interaction. Importantly, the Au-Au distance in **4**, 3.518(1) Å, is shorter than the length of 3.544 Å in **5a**. It might have been expected that the Au-Au distance would lengthen as the more electronegative Cl[−] replaced the Br[−] ligand on the [Au(bpy)Cl₂]⁺ unit because the Cl atom would withdraw more electron density than Br, forming a weaker metallophilic interaction.^[42] Based on the shortened Au-Au distance, however, it appears that the smaller size of the Cl atom plays a larger role than its greater electronegativity, compared to Br, in this aurophilic interaction.

Another observation that should be noted about **4** is a difference in empirical formulae observed in elemental analysis (C₁₀H₈N₂Cl₂Br₄Au₂) versus that used in the X-ray diffraction solution (C₁₀H₈N₂Cl_{0.76}Br_{5.24}Au₂). These data suggest that halide exchange is occurring in the compound, probably during recrystallization. Although the compound has an overall empirical formula of C₁₀H₈N₂Au₂Cl₂Br₄, the Br:Cl ratio in a single crystal may not be consistent with this overall proportion.

Synthesis of the mixed valence [Au(bpy)Cl₂][Au(CN)₂] double salt, **6**, was carried out analogously via the path C metathesis in Scheme 6 of **1** and KAu(CN)₂. Compound **6** is a pale yellow powder but due to limited solubility in CH₃CN and DMSO, crystals for X-ray diffraction could not be obtained. Elemental analysis data confirm the proposed stoichiometry.

Future preparations of [Au(III)]⁺[Au(I)][−] double salts are planned with [AuX₂][−] anions in which X = Cl or Br. The (R₄N)[AuX₂] salts are readily prepared from Au(III) reagents with mild reducing agents such as hydrazine.^[43] Reduction of Au(III) to Au(I) can also be effected by organic solvents such as acetone^[43] or other organic reagents including Na(acac).^[44] We have successfully used this chemistry to prepare [Pt(II)]⁺[Au(I)][−] double salts from [Pt(II)]⁺ and [Au(III)][−] reagents as described subsequently. This in situ reduction route from Au(III)/Au(III) to Au(III)/Au(I) shows much promise for compounds of the structure type [Au(R₂bpy)X₂][AuX₂] as an alternative route to metathesis reactions with the R₄N[AuX₂] salts.

GOLD COMPOUNDS: SPECTROSCOPY

In all Au(III)-Au(III) double salt complexes, the UV-vis spectra are dominated by the UV bipyridine $\pi - \pi^*$ and visible Au(III)-bipyridine MLCT transitions. Whereas in **3** the spectrum is a superposition of its cationic and anionic components, this phenomenon is not observed in the spectra of **4** and **5**.

As shown in Figure 4, the green curve, **3**, exhibits a λ_{\max} at 276.0 nm, which is nearly identical to the absorption wavelength of 275.6 nm belonging to the blue curve for the cationic component $[\text{Au}(\text{bpy})\text{Cl}_2]^+$. The extinction coefficient in the region between 300–350 nm is larger in the spectrum of **3** versus **1**, possibly indicating a superposition of the shifted KAuCl_4 LMCT transition since the λ_{\max} for the anionic component is observed at 323.0 nm, shown in purple on the graph.

However, in the case of **5** there is less blue shift of the $[\text{AuBr}_4]^-$ LMCT, as shown in Figure 5. The λ_{\max} for KAuBr_4 occurs at 396.0 nm, and the λ_{\max} for **5** is blue shifted to only 355.0 nm. Although the compound $[\text{Au}(\text{bpy})\text{Br}_2]\text{Br}$ could not be isolated, the additional band in

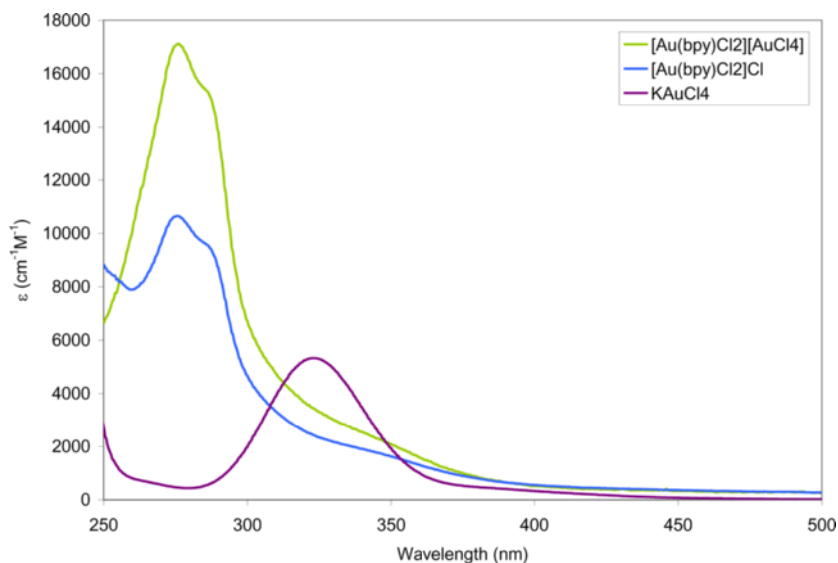


Figure 4. UV-vis spectra of **3** in CH_3CN . The double salt components $[\text{Au}(\text{bpy})\text{Cl}_2]^+$ and $[\text{AuCl}_4]^-$ are included for comparison.

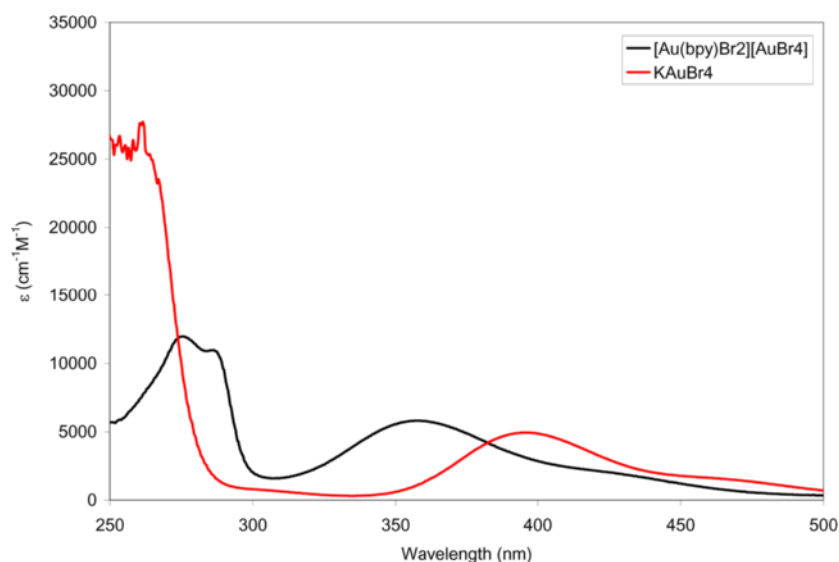


Figure 5. UV-vis spectra of **5** in CH_3CN . The double salt component KAuBr_4 is included for comparison.

the spectrum of **5** can be interpreted as resulting from the cationic species since its shape and relative λ_{max} are similar to those for **1**.

The spectrum for **4** (Figure 6) also displays a lack of complete superposition of the isolated cation, **1**, and anion species, KAuBr_4 , on the double salt. The λ_{max} for **4** is red shifted to 309.0 nm from the λ_{max} for the cationic species, observed at 275.6 nm. The energy of the transition near 400 nm in KAuBr_4 is unshifted in the double salt **5**. Notably, there are two flanking shoulders at approximately 297 nm and 325 nm, located on the sides of the band at 309.0 nm. These bands may belong to $[\text{AuCl}_4]^-$ and $[\text{Au}(\text{bpy})\text{Br}_2]^+$, produced by the halide exchange described previously. The absorbance at 325 nm would correspond with $[\text{AuCl}_4]^-$ because KAuCl_4 exhibits a band at 323.0 nm. The absorbance of 297 nm, shown in Figure 5, is also similar to the band in the spectrum for **5**, which is assumed to belong to the $[\text{Au}(\text{bpy})\text{Br}_2]^+$ component of the double salt.

The UV-vis spectrum of the Au(III)-Au(I) double salt complex **6** is also dominated primarily by the UV bipyridine $\pi-\pi^*$ and visible Au(III)-bipyridine MLCT transitions. The spectrum for **6** shows a superposition of its cationic and anionic components. The MLCT band in **6** is

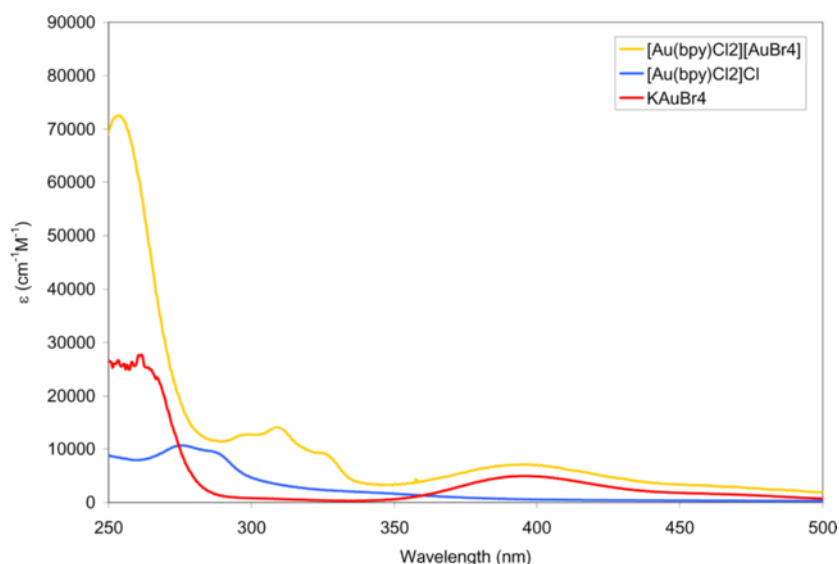
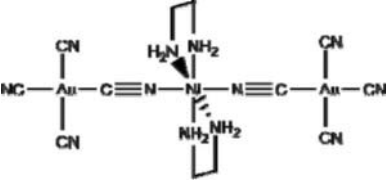
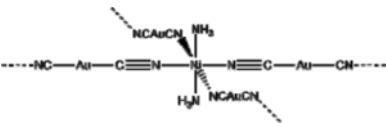


Figure 6. UV-vis spectra of **4** in CH₃CN. The double salt components **1** and KAuBr₄ are included for comparison.

located at a λ_{\max} of 314.1 nm and the $\pi - \pi^*$ transition is observed at 284.9 nm. These data suggest that in the cases of **3–5**, some cation anion interaction is present in solution that perturbs the LMCT bands in the $[\text{AuX}_4]^-$ anions. A metallophilic interaction in solution that affects the Au orbital energies is possible and is under further investigation.

Because structural characterization of **6** could not be obtained, the presence of an Au-Au interaction was probed indirectly via infrared spectroscopy. The vibrational frequency of the $\text{C}\equiv\text{N}$ stretch in **6** could be significantly different if the cyanide ligand binds in a terminal fashion to the Au(I) center versus a bridging cyanide mode. A series of cyanide stretches from gold cyanide species are presented in Table 1. The frequency for the $\text{C}\equiv\text{N}$ stretch in $\text{KAu}(\text{CN})_2$ occurs at 2141 cm^{-1} ^[45] and the $\text{C}\equiv\text{N}$ stretch occurs at 2189 cm^{-1} in $\text{KAu}(\text{CN})_4$.^[46] In some bridging cyanide complexes, the cyanide band has been observed to shift to higher energy values such as 2214 cm^{-1} and 2202 cm^{-1} , as seen in the compound $[\text{Ni}(\text{en})_2][\text{Au}(\text{CN})_4]_2$,^[46] and 2174 cm^{-1} in the case of $[\text{Ni}(\text{NH}_3)_2][\text{Au}(\text{CN}_2)_2]$.^[47] This trend is not always observed in gold compounds, however, due to the weakness of gold in π -back bonding.^[48] In **6** the $\text{C}\equiv\text{N}$ vibrational stretch occurs at 2218 cm^{-1} , which seems high for a

Table 1. C≡N stretching frequencies in Au(III) and Au(I) Cyanometalates

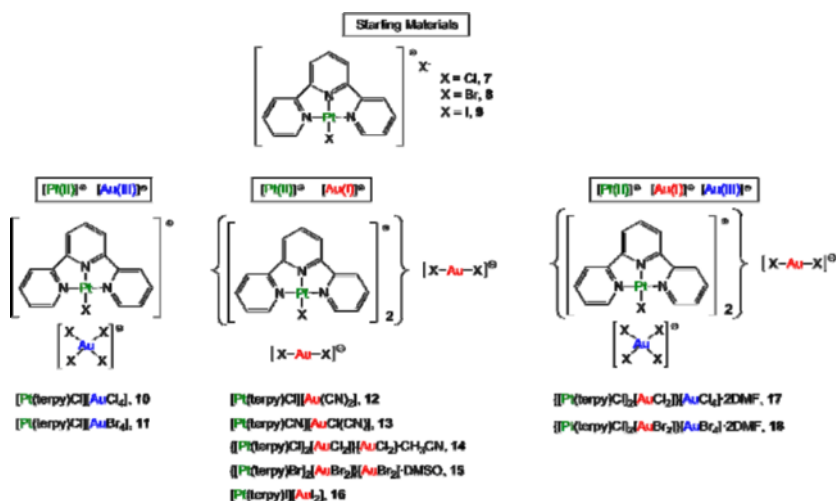
Compound	Bonding mode	ν (cm ⁻¹)	Reference
KAu(CN) ₂		2141	45
KAu(CN) ₄		2189	46
	bridging, terminal	2214, 2202, 2190, 2180	46
	bridging	2174	47
[Au(bpy)Cl ₂][Au(CN) ₂], 6	bridging (?)	2218	39

bridging rather than terminal cyanide mode, and still awaits structural confirmation. IR studies of the non-bridging [Au(CN)₂]⁻ and [AuCl(CN)]⁻ anions with platinum-based cations have significantly lower C≡N frequencies near ~ 2100 cm⁻¹, *vide infra*.

PLATINUM COMPOUNDS: SYNTHESIS AND STRUCTURAL CHARACTERIZATION

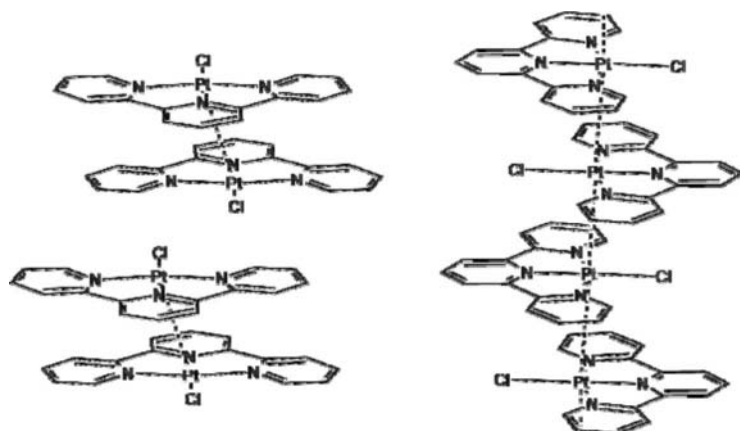
The second family of double salts described herein is based on [Pt(terpy)X]⁺ cations. A summary of the platinum-containing cations and the compounds prepared from them is presented in Scheme 7. All the compounds contain Pt(II) cations and are categorized according to the anion oxidation state: Au(III) on the left, Au(I) in the center, and mixed Au(III) and Au(I) on the right.

As with the gold cation-based systems, crystallographic analysis of the platinum starting materials is informative. We have reported that [Pt(terpy)Cl]Cl, 7, crystallizes with different solid state stacking, depending on the solvent from which it was crystallized.^[49] Shown in Scheme 8 are the arrangements observed with recrystallization from



Scheme 7. Summary of platinum-containing cations and metallophilic double salts.

H₂O and DMSO. Shown on the left is the cation-cation stacking pattern observed in a yellow polymorph upon recrystallization from water. Pairwise metallophilic attractions are observed between Pt centers at a distance of 3.3903(5) Å the van der Waals radius of Pt being

Scheme 8. Comparison of stacking patterns for 7 recrystallized from H₂O (left) and DMSO (right).

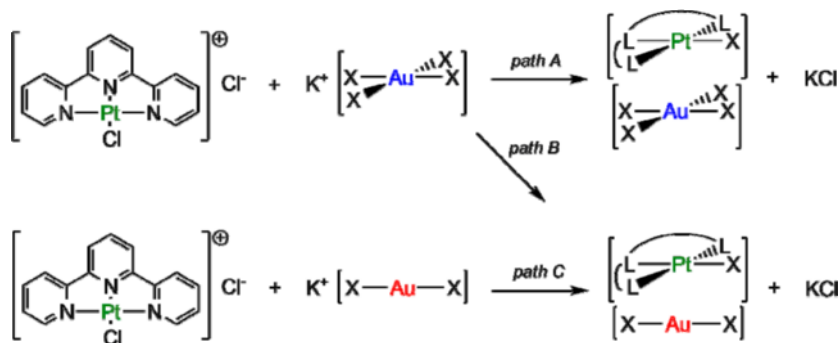
1.75 Å,^[18] but no extended network is observed. In contrast, a red polymorph is obtained from DMSO that exhibits an infinite chain of Pt···Pt contacts at alternating distances of 3.3155(8) and 3.4360(8) Å. The red color is indicative of {Pt···Pt···}_∞ bonding as has been previously reported in the [Pt(bpy)Cl₂] red^[50] and yellow^[51] polymorphs. The alternation of short and long M···M contacts in this case may be attributed to a Peierls distortion, which have been more frequently investigated in mixed-valent halogen bridged Pt(II)-X-Pt(IV) systems.^[52,53] Again one sees that electrostatic repulsion does not prevent formation of metallophilic interactions, but other forces influence the final structure. In these two cases, the crystallization solvent plays a determining role.

The bromide and iodide derivatives of [Pt(terpy)X]X are readily prepared by halide exchange^[54] from [Pt(terpy)Cl]Cl and recrystallized from hot aqueous solutions, but have not been studied crystallographically.

Three synthetic methodologies were employed for the Pt-containing double salts and these are depicted in Scheme 9. As with the [Au(bpy)X₂]⁺ derivatives, the paths A and C metathesis routes are most straightforward and potentially afford the greatest variety of products. In compounds containing [AuX₂][−], however, some species were best obtained through an indirect route, path B.

[Pt(II)]⁺[Au(III)][−] Double Salts

Two [Pt(II)]⁺[Au(III)][−] compounds were obtained by the metathesis route. The reaction of [Pt(terpy)Cl]Cl, **7**, with K[AuX₄] in water was



Scheme 9. Pathways to [Pt]⁺[Au][−] double salts.

successful in preparing both the chloride and bromide derivatives, $[\text{Pt}(\text{terpy})\text{Cl}][\text{AuCl}_4]$, **10**, and $[\text{Pt}(\text{terpy})\text{Cl}][\text{AuBr}_4]$, **11**. The former compound is pale yellow and the latter is tan, and the compositions were confirmed by elemental analysis. Structural data were not obtained, however, because of difficulties in recrystallization. Crystals of both compounds from CH_3CN were too small for single-crystal diffraction experiments without synchrotron radiation. When dissolved in DMSO or DMF, color changes were observed and the products recrystallized from these solutions were found to have undergone partial reduction of Au(III) to Au(I), forming species with $\{\text{Pt}(\text{II})_2\text{Au}(\text{III})\text{Au}(\text{I})\}$ stoichiometries, *vide infra*.

$[\text{Pt}(\text{II})]^+[\text{Au}(\text{I})]^-$ Double Salts

Platinum double salts with Au(I) were also synthesized via metathesis, path C, including $[\text{Pt}(\text{terpy})\text{Cl}][\text{Au}(\text{CN})_2]$, **12**, which was isolated as yellow-orange powder. The crystal structure of **12** (Figure 7) shows that only $\text{Pt} \cdots \text{Au}$ interactions are present, with no $\text{Pt} \cdots \text{Pt}$ or $\text{Au} \cdots \text{Au}$ contacts. The $\text{Pt}(\text{II}) \cdots \text{Au}(\text{I})$ distances are $3.349(1) \text{ \AA}$, required by symmetry to be equivalent, and are shorter than the sum of the apposite van der Waals radii, 3.41 \AA .^[55]

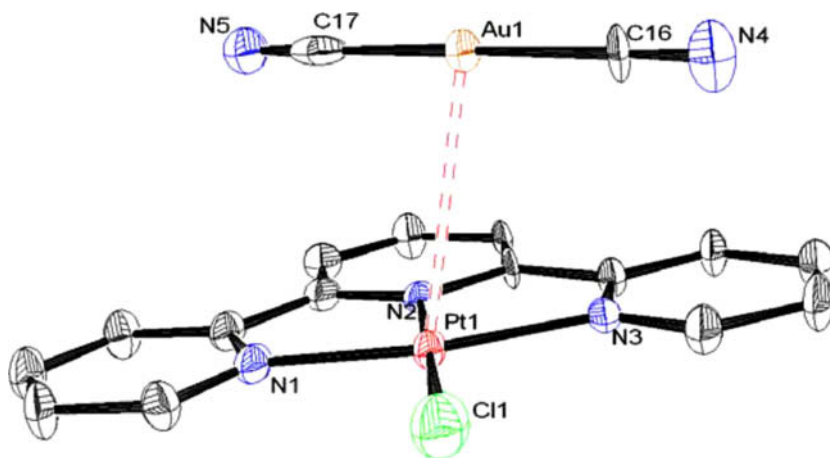


Figure 7. ORTEP of $[\text{Pt}(\text{terpy})\text{Cl}][\text{Au}(\text{CN})_2]$, **12**, with 50% ellipsoid probability and hydrogen atoms omitted for clarity).

These interactions are not perfectly linear, however. As seen in Figure 8, due to crystal packing forces each terpyridine ring is in close proximity to the adjacent $[\text{Au}(\text{CN})_2]^-$ anion. The result is a significant bend in the chain with a $\text{Pt}(1)\text{--Au}(1)\text{--Pt}(1)$ angle of 127.83° . There are no additional molecules in the lattice adjacent to the metallophilic chain to prevent this close packing and the result is an infinite chain of metallophilically bonded alternating cations and anions running through the crystal.

Recrystallization of $[\text{Pt}(\text{terpy})\text{Cl}][\text{Au}(\text{CN})_2]$ from hot acetonitrile yielded ruby red crystals, in contrast to the red-brown ones of **12**. X-ray diffraction studies showed that the ruby red crystals were the isomeric $[\text{Pt}(\text{terpy})\text{CN}][\text{AuCl}(\text{CN})]$, **13** (Figure 9), presumably formed by ligand exchange between the cation and anion. Similar behavior was observed in the recrystallization of compound **4**, *vide supra*. The cation $[\text{Pt}(\text{terpy})\text{CN}]^+$ had been previously reported and characterized spectroscopically,^[56,57] but this structure constituted the first report of the $[\text{AuCl}(\text{CN})]^-$ anion.^[39] The structure of **13** is quite similar to that of **12**, as shown in Figure 9. In $[\text{Pt}(\text{terpy})\text{Cl}][\text{AuCl}(\text{CN})]$ the $\text{Pt}\cdots\text{Au}$ contact is 3.340 \AA , slightly shorter than 3.349 \AA in $[\text{Pt}(\text{terpy})\text{Cl}][\text{Au}(\text{CN})_2]$, **12**. The effect of cyanide replacement by chloride is a slightly more

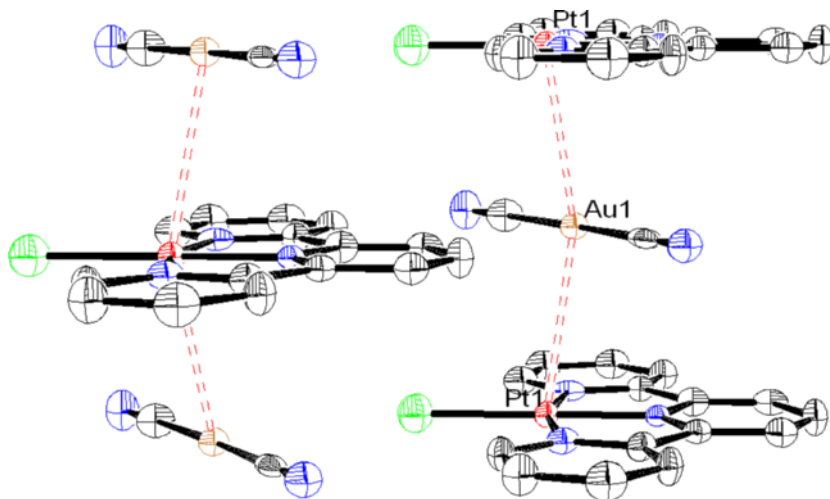


Figure 8. Selected packing in $[\text{Pt}(\text{terpy})\text{Cl}][\text{Au}(\text{CN})_2]$, **12**, with 50% ellipsoid probability and hydrogen atoms omitted for clarity.

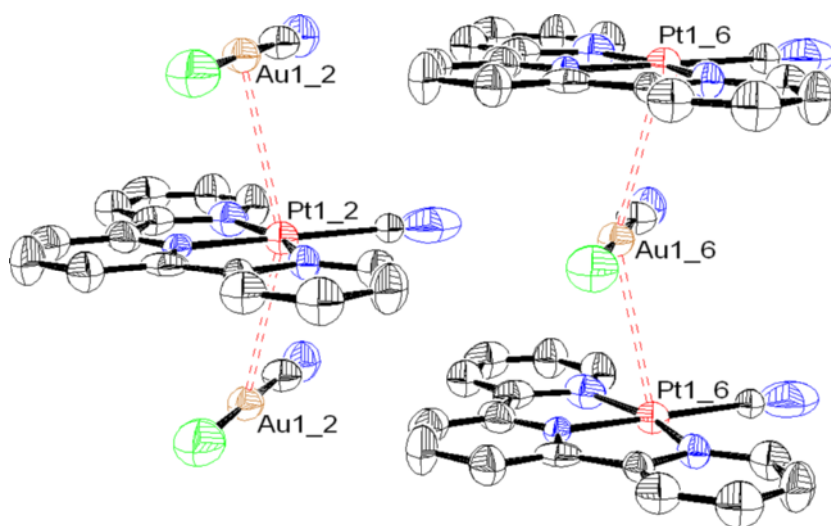


Figure 9. Selected packing in $[\text{Pt}(\text{terpy})\text{CN}][\text{Au}(\text{Cl})\text{CN}]$, **13**, with 50% ellipsoid probability and hydrogen atoms omitted for clarity.

electron rich gold center to interact with the platinum leading to a shorter $\text{M} \cdots \text{M}$ distance. As a result of the ligand changes from **12** to **13**, the Au(I) center may have become more electron rich for a metallophilic interaction with Pt(II), but simultaneously, the Pt(II) atom has become less so, such that no substantial change in the $\text{M} \cdots \text{M}$ distance occurs.

We have also prepared $[\text{Pt}(\text{II})]^+[\text{Au}(\text{I})]^-$ double salts with Au(I) anions from Au(III) starting materials. The series of compounds $[\text{Pt}(\text{terpy})\text{X}][\text{AuX}_2]$ where $\text{X} = \text{Cl}$ (**7**),^[39] Br (**8**),^[58] or I (**9**)^[59] have been prepared and crystallographically characterized. Their structures are particularly informative with regard to steric and electronic factors in forming metallophilic $\text{Pt} \cdots \text{Au}$ interactions. Unlike **12** and **13**, all the cations and anions in the $[\text{Pt}(\text{terpy})\text{X}][\text{AuX}_2]$ structures are not observed in a single 1D chain. Instead two different motifs are observed. The chloride and bromide derivatives have analogous structures containing an infinite chain of $\{[\text{Pt}(\text{terpy})\text{X}]_2[\text{AuX}_2]\}^+$ cations held together via metallophilic interactions. In contrast, the iodide compound does not have any linear chains, as discussed below.

The compound $\text{Et}_4\text{N}[\text{AuCl}_2]$ was prepared^[39] by phenylhydrazinium chloride reduction of $\text{Et}_4\text{N}[\text{AuCl}_4]$.^[43] Reaction of this salt with

[Pt(terpy)Cl]Cl in absolute ethanol led to the desired [Pt(terpy)Cl][AuCl₂], **14**. Minimizing the water present is critical with Au(I) dihalide anions to prevent disproportionation into Au(III) and Au(0).

The crystal structure of **14** consists of a [AuCl₂][−] anion sandwiched between two [Pt(terpy)Cl]⁺ cations to give a [Pt–Au–Pt]⁺ positively charged complex as shown in Figure 10. The other [AuCl₂][−] anion is adjacent to the [Pt–Au–Pt]⁺ cation but not bonded to it. Pt(II)···Au(I) interactions are present in the [Pt–Au–Pt]⁺ cationic complex at 3.268 Å, less than the sum of the van der Waals radii of platinum and gold, 3.41 Å.^[55] The Pt(1)–Au(1)–Pt(1–2) angle is linear due to the symmetry of the crystal. The two platinum cations are arranged head to tail with the [AuCl₂][−] anion in between as seen on the right side of Figure 10.

The [Pt(II)₂Au(I)]⁺ cations overcome Coulombic repulsion and stack in a near linear fashion to create Pt(II)···Pt(II) interactions as well, as shown in Figure 11. Rather than interacting with a gold atom to give a {Pt(II)···Au(I)}_∞ chain of interactions, the platinum atoms at the end of the [Pt–Au–Pt]⁺ cationic complex interact with other [Pt–Au–Pt]⁺ cations. As a result, an infinite chain of metallophilic interactions is present throughout the compound in a {Pt(II)···Au(I)···Pt(II)}_∞ array. The Pt(II)···Pt(II) interaction is evident in the crystal structure although the internuclear distance, 3.447 Å, is close to the sum of two platinum van der Waals radii, 3.50 Å.⁵⁵ The Pt(1)–Pt(1–2)–Au(1) angle resulting from the nonlinear stacking of the [Pt–Au–Pt]⁺ cationic complex is 145.1°. This bending may be the result of steric pressure from

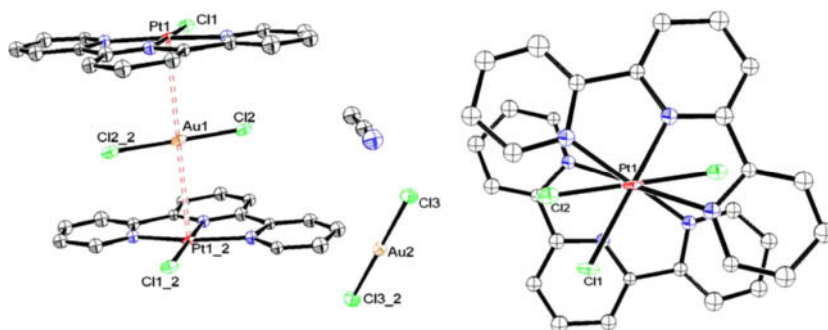


Figure 10. ORTEP of [Pt(terpy)Cl][AuCl₂], **14** with lattice CH₃CN (left) and view of the {[Pt(terpy)Cl]₂[AuCl₂]}⁺ cation (right) with 50% ellipsoid probability and hydrogen atoms omitted for clarity.

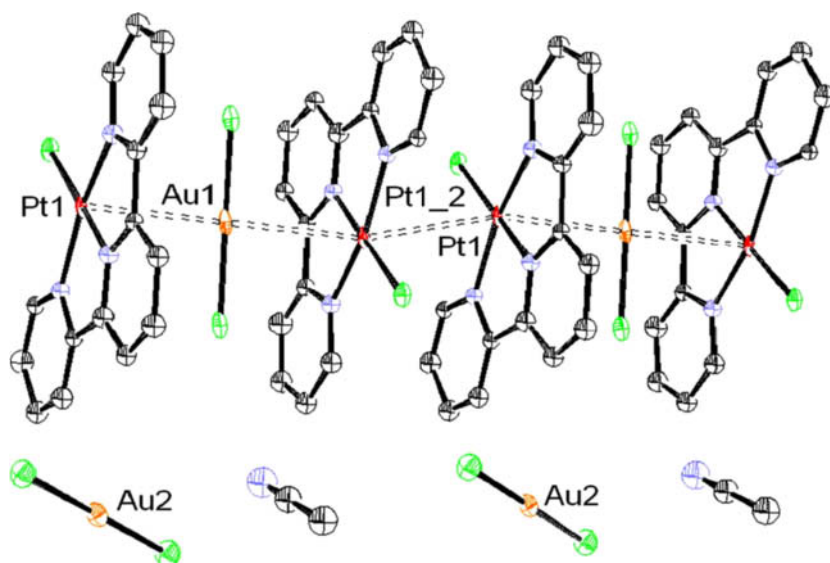


Figure 11. ORTEP of stacking in $[\text{Pt}(\text{terpy})\text{Cl}][\text{AuCl}_2] \cdot \text{CH}_3\text{CN}$, **14**, with 50% ellipsoid probability and hydrogen atoms omitted for clarity.

the molecules adjacent to the $\{\text{Pt}(\text{II}) \cdots \text{Au}(\text{I})\}_\infty$ chain, electrostatic attraction of the cationic complexes with the $[\text{AuCl}_2]^-$ anion, or π -interactions between the terpyridine ligands on platinum. A molecule of CH_3CN is also present in the asymmetric unit.

It is notable that such an unusual structure results simply from the replacement of cyanide on Au in $[\text{Pt}(\text{terpy})\text{Cl}][\text{Au}(\text{CN})_2]$, **12**, to chloride on Au in $[\text{Pt}(\text{terpy})\text{Cl}][\text{AuCl}_2]$, **14**. In **12**, the platinum and gold atoms alternate in a chain to form only $\{\text{Pt}(\text{II}) \cdots \text{Au}(\text{I})\}_\infty$ interactions, as shown before in Figure 8, but in **14** there is an infinite chain of $\{\text{Pt}(\text{II}) \cdots \text{Au}(\text{I}) \cdots \text{Pt}(\text{II})\}_\infty$ contacts. The difference in the arrangement is most likely caused by the change in electron density at the Au center resulting from the electronic differences between the chloride and cyanide ligands.

The bromide analog $[\text{Pt}(\text{terpy})\text{Br}][\text{AuBr}_2]$, **15**, is structurally very similar to the chloride derivative. It was prepared^[58] by reaction of $[\text{Pt}(\text{terpy})\text{Br}]\text{Br}$ with KAuBr_4 in room temperature acetone under which conditions Au(III) is reduced to Au(I) and monobromoacetone is a byproduct. $(\text{Et}_4\text{N})[\text{AuBr}_2]$ is produced from $(\text{Et}_4\text{N})[\text{AuBr}_4]$ under such conditions^[43] and therefore this synthesis bypassed the need to prepare $(\text{Et}_4\text{N})[\text{AuBr}_2]$ independently. Again, the structure consists of infinite

chains of the trimeric cations $\{[\text{Pt}(\text{terpy})\text{Br}]_2[\text{AuBr}_2]\}^+$ held together by metallophilic interactions, as shown in Figure 12. Charge balance is maintained by the remaining equivalent of $[\text{AuBr}_2]^-$ that is not part of the chain and a molecule of the DMSO recrystallization solvent fills out the space in the lattice. The most notable features are the Pt-Au distances within the cation. These are shorter (3.433 Å) than those in the chloride derivative **14** (3.453 Å). The studies of halide variation in metallophilic systems have demonstrated that metallophilic interactions are shorter with the less electronegative halide ligands.^[42] This is understood as an increase in electron density at the metal center, which strengthens the dispersion interaction and is consistent with the differences observed between **14** and **15**.

The compound $[\text{Pt}(\text{terpy})\text{I}][\text{AuI}_2]$, **16**, was prepared^[59] to complete this comparison of the effects on metallophilic interactions by changing the halide anion. Metathesis of $[\text{Pt}(\text{terpy})\text{I}]\text{I}$ and $(\text{Et}_4\text{N})[\text{AuI}_2]$ in absolute ethanol was used analogous to **14**. The iodide compound **16** does not have infinite chains of any kind but only exhibits pairwise metallophilic interactions between two $[\text{Pt}(\text{terpy})\text{I}]^+$ ions and no metallophilic

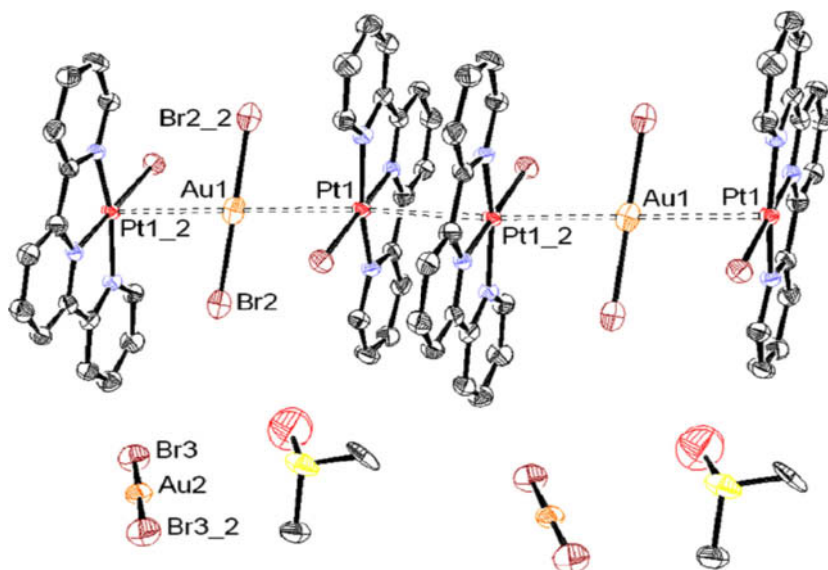


Figure 12. ORTEP of $\{[\text{Pt}(\text{terpy})\text{Br}]_2[\text{AuBr}_2]\}[\text{AuBr}_2]$ and DMSO with thermal ellipsoids at 50% level and hydrogen atoms removed for clarity.

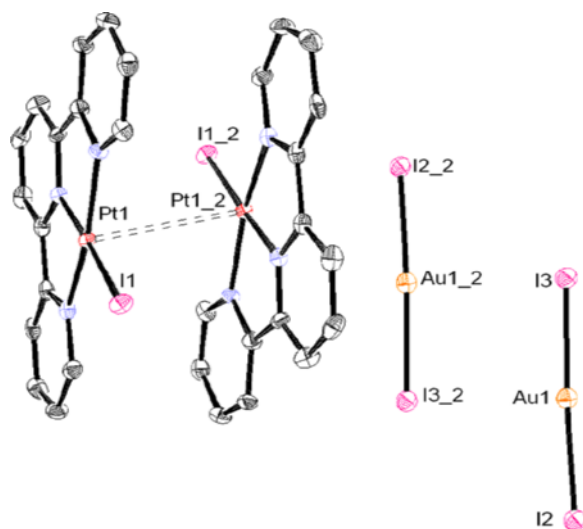


Figure 13. ORTEP of $[\text{Pt}(\text{terpy})\text{I}][\text{Au}(\text{I})_2]$, 16, with ellipsoids at the 50% level and hydrogen atoms removed for clarity.

interactions involving the $[\text{AuI}_2]^-$ anion are present, as shown in Figure 13. The $\text{Pt} \cdots \text{Pt}$ contact is $3.5279(5) \text{ \AA}$ long and slightly longer than twice the Pt van der Waals radius (3.50 \AA). To our knowledge, there is only one structurally characterized example of a metallophilic interaction between $[\text{AuI}_2]^-$ anions, which was observed in the presence of a methyl viologen dication, as depicted in Scheme 2.^[29] Critically, there are no observed examples of $[\text{AuI}_2]^-$ in a metallophilic interaction with an adjacent metal center that is not two-coordinate. The lack of such an interaction is due to the greater van der Waals radius of iodide than Au(I) such that other metal atoms can only approach the gold center closely if they do not overlap the iodide. Thus this anion is not a suitable counterpart for nanowire formation with $[\text{PtL}_3\text{X}]^+$ or $[\text{AuL}_2\text{X}_2]^+$ cations.

$[\text{Pt}(\text{II})]_2^+ [\text{Au}(\text{I})][\text{Au}(\text{III})]^-$ Double Salts

As mentioned previously, under certain recrystallization conditions, $[\text{Pt}(\text{II})]^+[\text{Au}(\text{III})]^-$ salts were observed to undergo some reduction at Au(III). Interestingly, this reduction is partial and resulted in salts with $[\text{Pt}(\text{II})]_2[\text{Au}(\text{III})][\text{Au}(\text{I})]$ stoichiometries. Recrystallization of $[\text{Pt}(\text{terpy})\text{Cl}][\text{AuCl}_4]$, 10, from DMF produces a mixture of red block-like crystals

and yellow needle-like crystals. The yellow crystals turned out to be the dihydrate of $[\text{Pt}(\text{terpy})\text{Cl}]\text{Cl}$, compound 7.^[49] X-ray diffraction showed that the more interesting red crystals were of $[\text{Pt}(\text{terpy})\text{Cl}]_2[\text{AuCl}_2][\text{AuCl}_4]$, 17, with two equivalents of DMF in the lattice as shown in Figure 14. Apparently half of the Au(III) was reduced to Au(I) to give the $[\text{AuCl}_2]^-$ anion. The formation of 7 may be related to the loss of chloride ions from the reduction of $[\text{AuCl}_4]^-$ to $[\text{AuCl}_2]^-$, which leaves an excess of chloride ions, however, the mechanism of the redox reaction is unknown. The most probable reductant of gold is the DMF, which partially reduced the Au(III) and was itself oxidized.

The crystal structure of 17 in Figure 14 shows a chain of metallophilic interactions in which the $[\text{AuCl}_2]^-$ anion is sandwiched between two $[\text{Pt}(\text{terpy})\text{Cl}]^+$ complexes to give $\text{Pt(II)} \cdots \text{Au(I)}$ interactions as observed in 14. The Pt(1)–Au(1) distance is 3.2834(15) Å, shorter than the sum of their van der Waals radii, 3.41 Å.^[55] Notably, the Au(III) in $[\text{AuCl}_4]^-$ is not bound to the $\text{Pt(II)} \cdots \text{Au(I)} \cdots \text{Pt(II)}$ system, but only maintains charge balance. The platinum interacts with the more electron rich Au(I) on one face and another $[\text{Pt}(\text{terpy})\text{Cl}]^+$ cation on the other. The Au(1) sits at an inversion center and therefore the $\text{Pt(II)} \cdots \text{Au(I)} \cdots \text{Pt(II)}$ interactions are perfectly linear. The entire chain of metal interactions, however, is not linear. The $[\text{Pt}–\text{Au}–\text{Pt}]^+$ cations are slightly offset giving

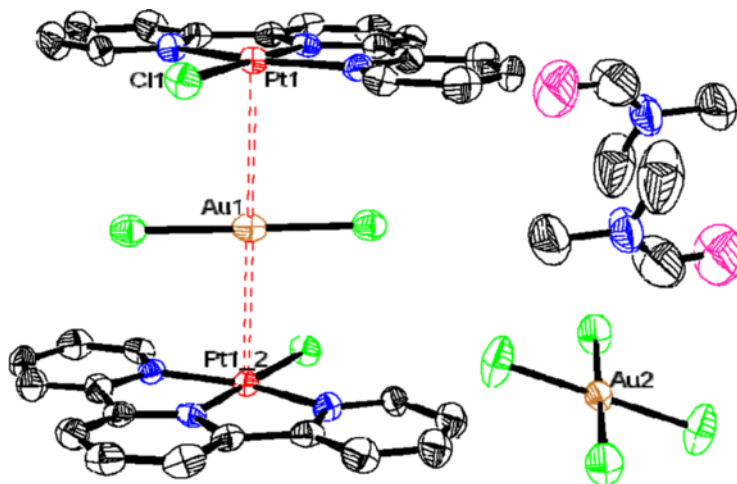


Figure 14. ORTEP of $[\text{Pt}(\text{terpy})\text{Cl}]_2[\text{AuCl}_2][\text{AuCl}_4]\cdot 2\text{DMF}$, 17, with 50% ellipsoid probability and hydrogen atoms omitted for clarity.

rise to a Pt(1)–Pt(1.2)–Au(1) angle of 150.58° , as shown in Figure 15. The kink in the chain may be the result of a several factors as discussed for compound 14.

With mixed valence gold atoms, $[\text{Pt}(\text{terpy})\text{Cl}]_2[\text{AuCl}_2][\text{AuCl}_4]$, 17, is similar to the pentanuclear compound $[\text{Au}(\text{terpy})\text{Cl}]_2[\text{AuCl}_2]_3[\text{AuCl}_4]$ synthesized by Hollis and Lippard.^[60] The difference in ion ratio is attributed to the variation in the charge of the $[\text{Pt}(\text{terpy})\text{Cl}]^+$ cation from the $[\text{Au}(\text{terpy})\text{Cl}]^{2+}$ dication. Unlike 17, the double salt by Hollis and Lippard was obtained by the reaction of HAuCl_4 with terpyridine in aqueous solution to synthesize $[\text{Au}(\text{terpy})\text{Cl}]\text{Cl}$. The double salt was a byproduct of the reaction and was pH dependent. Despite the similarities between 17 and $[\text{Au}(\text{terpy})\text{Cl}]_2[\text{AuCl}_2]_3[\text{AuCl}_4]$, their crystal structures differ significantly. In $[\text{Au}(\text{terpy})\text{Cl}]_2[\text{AuCl}_2]_3[\text{AuCl}_4]$, the chloride from

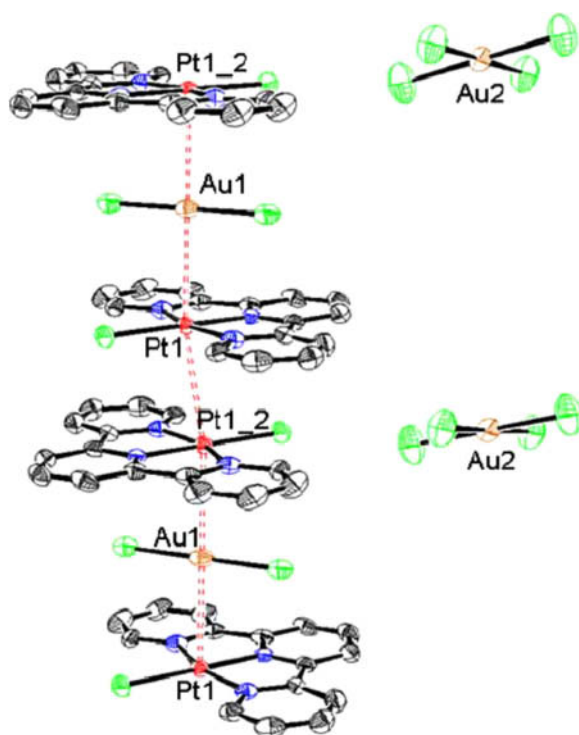


Figure 15. ORTEP of stacking in $[\text{Pt}(\text{terpy})\text{Cl}]_2[\text{AuCl}_2][\text{AuCl}_4]$, 17, with 50% ellipsoid probability and hydrogen atoms and DMF solvent molecules omitted for clarity.

the $[\text{AuCl}_4]^-$ anion bridges the gold in $[\text{Au}(\text{terpy})\text{Cl}]^{2+}$, as observed with $[\text{AuBr}_4]^-$ in **5b**, and terminates the chain of gold interactions instead of being alongside the chain of metallophilic interactions. Like **14**, however, only the $[\text{AuCl}_2]^-$ and not the $[\text{AuCl}_4]^-$ anion participates in a metallophilic interaction with the $[\text{M}(\text{terpy})\text{Cl}]^{n+}$ cation. Again, the metal center in $[\text{M}(\text{terpy})\text{Cl}]^{n+}$ seems to favor an interaction with Au(I) over Au(III) because Au(I) has more electron density for greater electron sharing between the metal atoms.

The analogous bromide complex, $[\text{Pt}(\text{terpy})\text{Cl}]_2[\text{AuBr}_2][\text{AuBr}_4] \cdot 2\text{DMF}$, **18**, was prepared by recrystallization of **11** from DMF. The crystal structure of **18**, shown in Figure 16, is similar to **17**, with a $[\text{AuBr}_2]^-$ complex sandwiched between two $[\text{Pt}(\text{terpy})\text{Cl}]^+$ cations and a $[\text{AuBr}_4]^-$ anion not bound to the $\{\text{Pt}(\text{II}) \cdots \text{Au}(\text{I}) \cdots \text{Pt}(\text{II})\}_\infty$ system. Again the positively charged $[\text{Pt}-\text{Au}-\text{Pt}]^+$ complex stacks in a near linear fashion to create an infinite array of $\{\text{Pt}(\text{II}) \cdots \text{Au}(\text{I}) \cdots \text{Pt}(\text{II})\}$ groups.

Thus there are two examples of the $\{\text{Pt} \cdots \text{Au}\}_\infty$ motif, **12** and **13**, and four examples of the $\{[\text{Pt}(\text{terpy})\text{X}]_2[\text{AuX}_2]\}_\infty^+$ motif. For the compounds containing the trinuclear cation, the important metrical parameters are compared in Table 2.

The most outstanding feature among the six compounds with infinite chains of metallophilic interactions is that in **12** and **13** all the metal atoms participate, but only three-quarters of the metal atoms participate in **14**, **15**, **17**, and **18**. In the former category, no Au(III) species are present and at least one cyanide ligand is bound to Au(I). Compounds

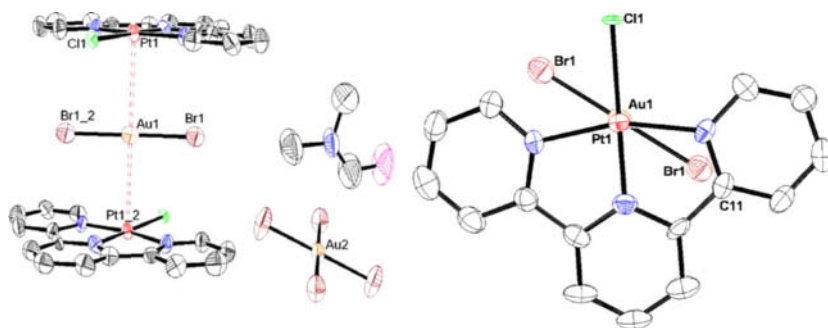


Figure 16. ORTEP of $[\text{Pt}(\text{terpy})\text{Cl}]_2[\text{AuBr}_2][\text{AuBr}_4] \cdot 2\text{DMF}$, **18** (left) and view of cation down *b*-axis (right) with 50% ellipsoid probability and hydrogen atoms removed for clarity.

Table 2. Metrical comparison of $\{[\text{Pt}(\text{terpy})\text{X}]_2[\text{AuX}_2]\}^+$ cations

Compound	Pt-X (Å)	Au(I)-X (Å)	Pt-Au (Å)	Pt-Pt (Å)	Au-Pt-Pt (°)
$\{[\text{Pt}(\text{terpy})\text{Cl}]_2[\text{AuCl}_2]\}[\text{AuCl}_2]$, 14	2.305(3)	2.271(3)	3.2683(5)	3.453(1)	165.10(3)
$\{[\text{Pt}(\text{terpy})\text{Cl}]_2[\text{AuCl}_2]\}[\text{AuCl}_4]$, 17	2.3034(19)	2.268(2)	3.2834(15)	3.447(1)	170.58(3)
$\{[\text{Pt}(\text{terpy})\text{Cl}]_2[\text{AuBr}_2]\}[\text{AuBr}_4]$, 18	2.367(2)	2.3962(18)	3.318	3.448	171.56
$\{[\text{Pt}(\text{terpy})\text{Br}]_2[\text{AuBr}_2]\}[\text{AuBr}_2]$, 15	2.4319(7)	2.3984(9)	3.336	3.433	173.94

14 and **15** also have only reduced Au(I) centers, but do not have any cyanide ligands. The absence of metallophilic interactions involving Au(III) is consistent with the fact that this ion has been the most recent to join the metallophilic family.^[38] Secondly, in **12** and **13** the {Pt-Au-Pt} angles are significantly non-linear due to steric pressure from adjacent chains. In contrast the structures of **14**, **15**, **17**, and **18**, contain solvent molecules and $[\text{AuX}_4]^-$ or $[\text{AuX}_2]^-$ anions separating the chains from one another. These additional species facilitate the linear arrangement of the {Pt-Au-Pt} angles within the $\{[\text{Pt}(\text{terpy})\text{X}]_2[\text{AuX}_2]\}^+$ cations.

The structure of **14** is quite similar to the structure of **17** in which it can be argued that the $\{\text{Pt(II)} \cdots \text{Au(I)} \cdots \text{Pt(II)}\}_\infty$ arrangement is due to a greater affinity of Pt(II) for Au(I) rather than Au(III). In **14**, however, the only oxidation states in the compound are Pt(II) and Au(I). The Pt(II) \cdots Pt(II) distances resulting from the stacking $[\text{Pt-Au-Pt}]^+$ cations in **14** are similar in magnitude to those of **17**. The Pt(II) \cdots Pt(II) distance in **14** is 3.453(1) Å, not significantly longer than 3.447(1) Å in **17**, which suggests that the anions external to these chains have little effect on the binding within the chains except perhaps for some steric pressure that affects the Au-Pt-Pt angles. The exclusion of the $[\text{AuCl}_2]^-$ anion from the chain in **14** suggests that the Pt \cdots Pt interaction is more favorable than another Pt \cdots Au metallophilic contact.

Upon changing from chloride to bromide, the Pt(II) \cdots Au(I) interaction is longer in **18** (3.318 Å) than in **17**, (3.28 Å). Previous studies^[42,61] have suggested that stronger metallophilic interactions are observed with more electron rich metals. In the case of **18**, incorporating a less electron withdrawing group on the gold has led to longer Pt \cdots Au contacts. There is a trend among the four compounds in Table 2 that as the Pt \cdots Au distance increases, the Pt \cdots Pt distance decreases, showing a subtle

interplay in the metallophilic interactions as a function of halide substitution. Thus the electron density on both the Pt and Au centers exert significant influence. Only with all four halogens changed to bromide in the $\{[\text{Pt}(\text{terpy})\text{X}]_2[\text{AuX}_2]\}^+$ cations is the greatest contraction of the Pt...Pt distance seen among these four compounds. Thus there is a competition for electron density between the Pt...Au metallophilic interaction within the cation and the Pt...Pt interactions between the cations.

When compared to the distances in **17** and **18**, 3.283(1) and 3.318(1) Å, the Pt...Au distance in **12**, 3.349(1) Å is noticeably longer. The longer distance is attributed to the cyanide groups on the gold atom. Unlike in **18**, steric bulk is not a factor in **12**, and the effect of putting more electron withdrawing groups on Au(I) can be observed. Putting a more electron withdrawing group, like cyanide, on the gold metal leaves the metal less electron rich for a metallophilic interaction.

PLATINUM COMPOUNDS: SPECTROSCOPY

The electronic spectrum of the starting material **7** had been recorded previously in water.^[62] Comparatively, the absorption spectrum of **7** in DMSO exhibits slightly different absorbances at 354, 335, 284, and 262 nm. The overall red shift of approximately 10 nm may be the result of Pt(II)...Pt(II) interactions that exist in DMSO but not water. In a dilute solution of DMSO, **7** gives an orange yellow color, while in aqueous solution it gives a pale yellow color. Recalling the crystal structure of $[\text{Pt}(\text{terpy})\text{Cl}]\text{Cl}$, Pt(II)...Pt(II) stacking interactions exist in the DMSO solvated red form but not in the dihydrate red-orange form.^[49] The formation of short Pt(II)...Pt(II) chains in DMSO could account for the color changes as has been reported previously for dimers or oligomers in platinum terpyridyl compounds.^[62,63]

The UV-vis spectra of the double salts containing $[\text{Pt}(\text{terpy})\text{X}]^+$ cations are all similar to the $[\text{Pt}(\text{terpy})\text{Cl}]^+$ cation and do not show any distinct features attributable to the presence of the anions or to metallophilic interactions^[39] as summarized in Figure 17. The spectra of **10** and **17**, which both contain the $[\text{AuCl}_4]^-$ anion, exhibit an extra shoulder around 365 nm perhaps due to the $[\text{AuCl}_4]^-$ anion (*cf* Figure 4). All other bands are from transitions in the $[\text{Pt}(\text{terpy})\text{Cl}]^+$ cation. No absorbances were observed in the region between 500 and 1100 nm. Bands typical of Pt-terpy MLCT^[54] are observed and an

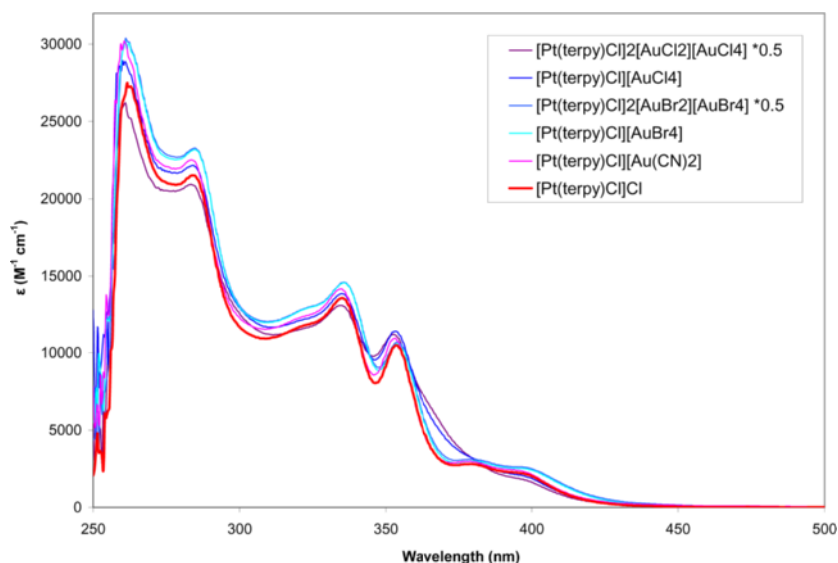


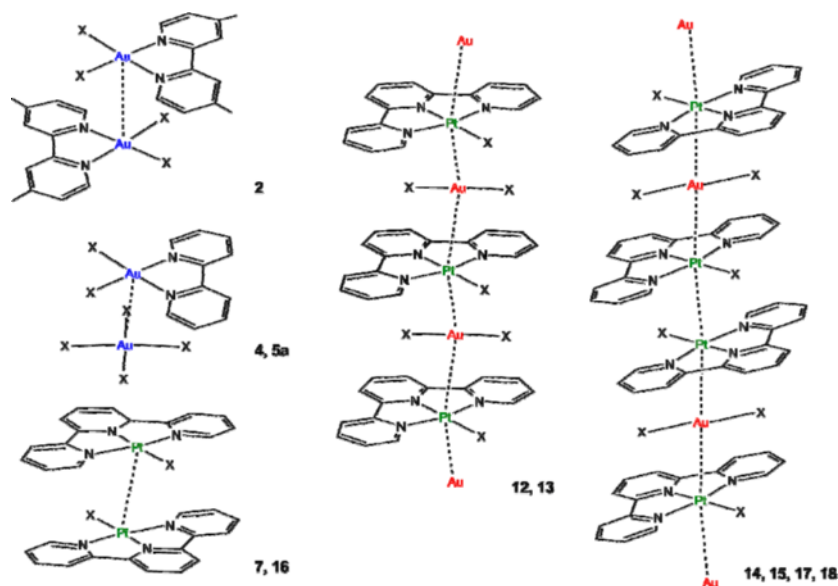
Figure 17. UV-Vis absorption spectra of platinum double salts 10–12, 14, and 15 compared to $[\text{Pt}(\text{terpy})\text{Cl}]\text{Cl}$, 7, in DMSO.

additional feature at 346 nm is seen only in the spectrum of 13 for the $[\text{Pt}(\text{terpy})\text{CN}]^+$ cation, consistent with the previously reported $[\text{Pt}(\text{terpy})\text{CN}](\text{OTf})$.^[57]

The IR spectra of 12 and 13 were collected in order to observe the cyanide stretching frequencies. Cyanide stretches of cyano gold compounds with the cyanide bridging two metals have been reported by Deeming and Hursthouse.^[64] For the compound $[(\text{PPh}_3)\text{Au}(\mu\text{-CN})\text{MCl}_2(\text{PMe}_2\text{Ph})_3]$, where $\text{M} = \text{Ir}$ or Rh , the cyanide stretches ranged from 2164 to 2204 cm^{-1} . Both 12 and 13 exhibit a $\text{C}\equiv\text{N}$ stretch at 2139 cm^{-1} , significantly lower than those reported for bridging cyanides,^[46,65] and consistent with the terminal mode determined crystallographically. The spectrum of 13 exhibits a second band at 2132 cm^{-1} due the cyanide ligand bound to platinum.

OUTLOOK AND FUTURE DIRECTIONS

A variety of different synthetic routes have yielded many new double salts with metallophilic interactions. Five different structural motifs have been



Scheme 10. Summary of observed metallophilic motifs in polyimine-containing compounds.

observed as depicted in Scheme 10. Metallophilic interactions with Pt(II) and Au(I) are clearly favored over those with Au(III). The potential for forming more related double salts is very high and is limited only by choice of X groups such that no bridging by, or steric hindrance from, X occurs.

There remain under-investigated spectroscopic questions. What are the solution and solid state luminescence properties of these compounds? Do the metallophilic interactions persist in solution by virtue of ion-pairing? Is there any concentration dependence to solution UV-vis or luminescence behavior? An obvious extension of these motifs is to paramagnetic starting materials with M having d^n , $n = \text{odd}$ electron configurations. In such circumstances, any metal-metal interactions could no longer be termed metallophilic, but would certainly be interesting compounds. The extensive work on partially oxidized platinum chains^[66,67] was explored with a similar idea in mind. Vigorous efforts are underway to synthesize more metallophilic 1D materials and develop methodologies for incorporating electronic structures that result in increased conductivity.

ACKNOWLEDGEMENTS

I would like to thank all my students and colleagues whose names appear in the references and whose enthusiasm, hard work, and dedication made these results possible. We are particularly grateful to the Rheingold group at UC San Diego for indefatigable crystallographic collaborations. For financial support we are indebted to NSF (CAREER to LHD CHE-0134817 and NSEC CHE-0117752 to Columbia University), the Dreyfus Foundation (New Faculty Award and Henry Dreyfus Teacher-Scholar Awards to LHD), Barnard College, and Boston University.

REFERENCES

1. Canadell, E. and M. H. Whangbo, 1991. *Chem. Rev.*, **91**, 965–1034.
2. Monthoux, P., D. Pines, and G. G. Lonzarich, 2007. *Nature*, **450**, 1177–1183.
3. Lescouezec, R., J. Vaissermann, C. Ruiz-Perez, F. Lloret, R. Carrasco, M. Julve, M. Verdager, Y. Dromzee, D. Gatteschi, and W. Wernsdorfer, 2003. *Angew. Chem., Int. Ed.*, **42**, 1483–1486.
4. Lescouezec, R., L. M. Toma, J. Vaissermann, M. Verdager, F. S. Delgado, C. Ruiz-Perez, F. Lloret, and M. Julve, 2005. *Coord. Chem. Rev.*, **249**, 2691–2729.
5. Toyota, N., M. Lang, and J. Müller, 2007. *Low Dimensional Molecular Materials*, Springer, Berlin.
6. Cassoux, P. and J. S. Miller, 1998. *Chemistry of Advanced Materials*, 19–72.
7. Miller, J. R. 1965. *J. Chem. Soc.*, 713–720.
8. Kauffman, G. B. 1976. *Platinum Met. Rev.*, **20**, 21–24.
9. Atkinson, L., P. Day, and R. J. P. Williams, 1968. *Nature*, **218**, 668–669.
10. Kim, E.-G., K. Schmidt, W. R. Caseri, T. Kreouzis, N. Stingelin-Stutzmann, and J.-L. Bredas, 2006. *Adv. Mater.*, **18**, 2039–2043.
11. Caseri, W. 2004. *Plat. Met. Rev.*, **48**, 91–100.
12. Drew, S. M., D. E. Janzen, C. E. Buss, D. I. MacEwan, K. M. Dublin, and K. R. Mann, 2001. *J. Am. Chem. Soc.*, **123**, 8414–8415.
13. Buss, C. E., C. E. Anderson, M. K. Pomije, C. M. Lutz, D. Britton, and K. R. Mann, 1998. *J. Am. Chem. Soc.*, **120**, 7783–7790.
14. Kittel, C. 2005. *Introduction to Solid State Physics*, John Wiley & Sons, Hoboken.
15. Ashcroft, N. W. and D. N. Mermin, 1976. *Solid State Physics*, Brooks/Cole, Boston.
16. Cotton, F. A., C. A. Murillo, and R. A. Walton, 2005. *Multiple Bonds Between Metal Atoms*, Springer, New York.
17. Pyykkö, P. 1997. *Chem. Rev.*, **97**, 597–636.
18. Bondi, A. 1964. *J. Phys. Chem.*, **68**, 441–451.

19. Mendizabal, F., P. Pykkö, and N. Runeberg, 2003. *Chem. Phys. Lett.*, **370**, 733–740.
20. Pykkö, P., N. Runeberg, and F. Mendizabal, 1997. *Chem. Eur. J.*, **3**, 1451–1457.
21. Mingos, D. M. P. 1996. *J. Chem. Soc., Dalton Trans.*, 561–566.
22. Doll, K., P. Pykkö, and H. Stoll, 1998. *J. Chem. Phys.*, **109**, 2339–2345.
23. Crespo, O., A. Laguna, E. J. Fernandez, J. M. Lopez de Luzauriaga, P. G. Jones, M. Teichert, M. Monge, P. Pykkö, N. Runeberg, M. Schultz, and H.-J. Werner, 2000. *Inorg. Chem.*, **39**, 4786–4792.
24. Mendizabal, F. and P. Pykkö, 2004. *Phys. Chem. Chem. Phys.*, **6**, 900–905.
25. Scherbaum, F., A. Grohmann, B. Huber, C. Krueger, and H. Schmidbaur, 1988. *Angew. Chem. Int. Ed. Engl.*, **27**, 1544–1546.
26. Schmidbaur, H. 2000. *Gold Bull.*, **33**, 3–10.
27. Ecken, H., M. M. Olmstead, B. C. Noll, S. Attar, B. Schlyer, and A. L. Balch, 1998. *J. Chem. Soc., Dalton Trans.*, 3715–3720.
28. Morsali, A. and R. Kempe, 2005. *Helv. Chim. Acta*, **88**, 2267–2271.
29. Tang, Z., A. P. Litvinchuk, H.-G. Lee, and A. M. Guloy, 1998. *Inorg. Chem.*, **37**, 4752–4753.
30. Green, M. L. H. 1995. *J. Organomet. Chem.*, **500**, 127–148.
31. Eryazici, I., C. N. Moorefield, and G. R. Newkome, 2008. *Chem. Rev.*, **108**, 1834–1895.
32. Harris, C. M. and T. N. Lockyer, 1959. *J. Chem. Soc.*, 3083–3085.
33. Hayoun, R., L. H. Doerrer, and A. L. Rheingold, 2005. *CSD Private Communication*, **266056**.
34. Bjernemose, J. K., P. R. Raithby, and H. Toftlund, 2004. *Acta Crystallogr. Sect. E*, **E60**, m1719–m1721.
35. McInnes, E. J. L., A. J. Welch, and L. J. Yellowlees, 1995. *Acta Cryst.*, **C51**, 2023–2025.
36. Ganzhi, M. and L. H. Doerrer, 2008. *Unpublished results*.
37. Allen, F. H. 2002. *Acta Cryst.*, **B58**, 380–388.
38. Klapötke, T. M., B. Krumm, J.-C. Galvez-Ruiz, and H. Noeth, 2005. *Inorg. Chem.*, **44**, 9625–9627.
39. Hayoun, R., D. K. Zhong, A. L. Rheingold, and L. H. Doerrer, 2006. *Inorg. Chem.*, **45**, 6120–6122.
40. Annibale, G., L. Cattalini, A. A. El-Awady, and G. Natile, 1974. *J. Chem. Soc., Dalton Trans.*, 802–807.
41. Hollis, S. L. and S. J. Lippard, 1983. *J. Am. Chem. Soc.*, **105**, 4293–4299.
42. Toronto, D. V., B. Weissbart, D. S. Tinti, and A. L. Balch, 1996. *Inorg. Chem.*, **35**, 2484–2489.
43. Braunstein, P. and R. J. H. Clark, 1973. *J. Chem. Soc., Dalton Trans.*, 1845–1848.

44. Buckley, R. W., P. C. Healy, and W. A. Loughlin, 1997. *Aust. J. Chem.*, **50**, 775–778.
45. Jones, L. H. 1957. *J. Chem. Phys.*, **27**, 468–472.
46. Shorrock, C. J., H. Jong, R. J. Batchelor, and D. B. Leznoff, 2003. *Inorg. Chem.*, **42**, 3917–3924.
47. Stender, M., R. L. White-Morris, M. M. Olmstead, and A. L. Balch, 2003. *Inorg. Chem.*, **42**, 4504–4506.
48. Schmidbaur, H., ed., 1999. *Gold: Progress in Chemistry, Biochemistry, and Technology*, John Wiley & Sons, New York.
49. Angle, C. S., A. G. DiPasquale, A. L. Rheingold, and L. H. Doerrer, 2006. *Acta Cryst.*, **C62**, m340–m342.
50. Osborn, R. S. and D. Rogers, 1974. *J. Chem. Soc., Dalton Trans.*, 1002–1004.
51. Textor, M. and H. R. Oswald, 1974. *Z. Anorg. Allg. Chem.*, **407**, 244–256.
52. Yamamoto, S. 2001. *Phys. Rev. B*, **64**, 140102/1–140102/4.
53. Yamamoto, S. and J. Ohara, 2007. *Phys. Rev. B*, **76**, 235116/1–235116/8.
54. Yip, H. K., L. K. Cheng, K. K. Cheung, and C. M. Che, 1993. *J. Chem. Soc., Dalton Trans.*, 2933–2938.
55. Bondi, A. 1964. *J. Phys. Chem.*, **68**, 441–451.
56. Mureinik, R. J. and M. Bidani, 1977. *Inorg. Nucl. Chem. Letters*, **13**, 625–629.
57. Wilson, M. H., L. P. Ledwaba, J. S. Field, and D. R. McMillin, 2005. *Dalton Trans.*, 2754–2759.
58. Kahn, M. I. and L. H. Doerrer, 2007. *Unpublished results*.
59. Angle, C. S., K. J. Woolard, M. I. Kahn, J. A. Golen, A. L. Rheingold, and L. H. Doerrer, 2007. *Acta Cryst.*, **C63**, m231–m234.
60. Hollis, L. S. and S. J. Lippard, 1983. *J. Am. Chem. Soc.*, **105**, 4293–4299.
61. Thomas, T. W. and A. E. Underhill, 1972. *Chem. Soc. Rev.*, **1**, 99–120.
62. Jennette, K. W., J. T. Gill, J. A. Sadownik, and S. J. Lippard, 1976. *J. Am. Chem. Soc.*, **98**, 6159–6168.
63. Bailey, J. A., M. G. Hill, R. E. Marsh, V. M. Miskowski, W. P. Schaefer, and H. B. Gray, 1995. *Inorg. Chem.*, **34**, 4591–4599.
64. Deeming, A. J., G. P. Proud, H. M. Dawes, and M. B. Hursthouse, 1988. *Polyhedron*, **7**, 651–657.
65. Stender, M., R. L. White-Morris, M. M. Olmstead, and A. L. Balch, 2003. *Inorg. Chem.*, **42**, 4504–4506.
66. Krogmann, K. 1969. *Angew. Chem., Int. Ed. Eng.*, **8**, 35–42.
67. Williams, J. M. and A. J. Schultz, 1979. *NATO Conference Series VI: Materials Science*, **1**, 337–368.